RSC Advances

ROYAL SOCIETY
OF CHEMISTRY

www.rsc.org/advances

Volatilization Interference on Thermal Analysis and Kinetics of

Low-melting Organic Nitro Compounds

Rui Liu, Tonglai Zhang[*], Zunning Zhou, Li Yang

State Key Laboratory of Explosion Science and Technology, School of Mechatronical Engineering, Beijing Institute of Technology, Beijing 100081, China

Volatilization interference is the first prerequisite to be eliminated for the quantitative thermal analysis of low-melting material. The volatilization processes of three low-melting organic nitro compounds, TNT, DNAN and DNTF, were measured by isothermal thermogravimetry. The thermal decomposition behaviors and kinetics were studied by dynamic pressure measuring thermal analysis. The interference of the vapor pressure on the gas pressure of thermal decomposition at specified temperatures was deducted quantitatively. DNAN is the most stable though three compounds all match the standard of good thermal stability. DNTF has the highest activity and most sensitive to heating under specified conditions. The surface changes caused by melting and thermal decomposition stimulate the reaction activity and affect the reaction kinetics and thermal stability. The reaction activity of the nitro compounds is directly related to the number of the nitro group / nitrogen atom.

Introduction

Low-melting organic nitro compounds (LONCs) are extensively used as the important insensitive energetic ingredients of the novel energy materials in military, defense and aerospace industries.[1,2] LONCs significantly improve the composite materials with better fluidity, stability and energy output because of their great advantages of high energy, low sensitivity, low vulnerability and low ablation.[3-5] Three typical LONCs, 2,4,6-trinitrotoluene (TNT), 2,4-dinitroanisole (DNAN) and 3,4-dinitrofurazanfuroxan (DNTF), are used widely in weapons and munitions, and have received some theoretical and experimental investigations.[6-9] Thermal analysis is very significant for LONCs to determine their thermal decomposition kinetics, mechanisms and thermal stability.[10-12] However, the volatilization of LONCs in applications interferes with the thermal analysis because it causes the changes of the characteristic parameters of thermal decomposition such as mass, pressure and heat. Therefore, the volatilization interference on thermal decomposition is the first prerequisite to be eliminated for the quantitative thermal analysis of LONCs.[13-15]

Most efforts have focused on exploring the workable methodologies for the vapor quantitative detection in the past decades. Many researches were carried out using the simple and direct manometer,[16,17] Knudsen and torsion effusion as well as gas saturation techniques at high temperature,[18-21] gas chromatography (GC) headspace technique,[22-24] DSC under high pressure in hermetic-type pan,[25,26] combination of electrodynamic balance and optical tweezers,[27] and volatility tandem differential mobility analyzer.[28] However, no feasible method has been established to adapt to the combination with thermal analysis until now, or seldom research has been paid attention to the researches of LONCs because their high-energy and sensitive properties could cause the lurking danger in tests. Thus, there are great challenges to determine the vapor pressures of LONCs and to exclude the volatilization interference on their thermal stability and reaction kinetics. Many analyses have proved that isothermal mass loss far below decomposition temperature approximates to a zero-order volatilization process.[29,30] Thermogravimetry (TG) provides a standard thermobalance and readily available sample holder. It requires low dose and ambient pressure, having the advantages of convenient operation and reliable measurement.[31,32] Isothermal TG is therefore a suitable tool for volatilization measurement. Among so many thermal analysis methods, pressure measuring methods, such as vacuum stability test and Bourdon manometry, are easy and safe to operate. They are used widely especially for the hazardous energetic materials. But these methods are the indirect and discontinuous measurements neither to display the entire decomposition process nor to determine the reaction kinetics. Dynamic pressure measuring thermal analysis (DPTA), formerly known as dynamic vacuum stability test (DVST), was established as a novel thermal analysis method by our group. DPTA can consecutively and directly record the absolute pressure changes caused by thermal decomposition. It has been successfully applied in the investigations of thermal stability and reaction kinetics for several energetic compounds.[33,34] Therefore, DPTA is a perfect replacement for the current pressure measuring methods.

In this work, the thermal volatilization processes of TNT, DNAN and DNTF were measured by TG and the thermal

decomposition behaviors were measured by DPTA. The enthalpies of sublimation and evaporation, and the

Clausius-Clapeyron equations were determined. The interference of the volatilization of the LONCs on the thermal

analysis was eliminated by means of the pressure data treatment. The thermal stability, reaction kinetics and mechanism
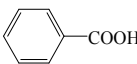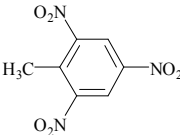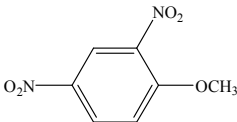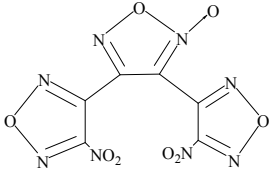
were determined as well.

Experimental

Materials

Benzoic acid with a high-purity of 99.97 % was used as a calibration substance in TG. Three LONCs, TNT, DNAN and

DNTF, have the same average particle size of *ca.* 80 μm. More information about the samples is detailed in **Table 1**.   To

avoid the influence of the adsorbed gaseous impurities   on the tests, the samples were vacuum-dried at   40 °C for 12 h

and then stored in a desiccator below room temperature before experiment.

Warning: TNT, DNAN and DNTF are hazardous energetic materials and therefore should be treated in small batches

with the proper safety protection.

Table 1 Information of samples used in this work

Sample	Structural formula	Source	Melting point (K)	Purity	Analysis method
Benzoic acid $C_7H_6O_2$	⬡—COOH	Sigma-Aldrich co.	395.55	> 0.9997	/
2,4,6-Trinitrotoluene (TNT) $C_7H_5N_3O_6$		Synthesis [a]	353.65	> 0.99	DSC [b]
2,4-Dinitroanisole (DNAN) $C_7H_6N_2O_5$		Synthesis	367.65	> 0.99	DSC
3,4-Dinitrofurazanfuroxan (DNTF) $C_6N_8O_8$		Synthesis	383.15	> 0.99	DSC

[a] The samples were provided by Xi'an Modern Chemistry Research Institute through synthesis, extraction, recrystallization and repurificaion.

[b] Melting point tested by DSC (differential scanning calorimetry).

Apparatus and Conditions

Pyris-1 model thermogravimetric analyzer (*Perkin-Elmer*, USA) was applied. About 10 mg of sample was spread thinly

and uniformly in an uncovered platinum crucible. Sample was heated from room temperature to target temperature at 10

K·min^{-1} and then kept isothermally over 15 h. Dry nitrogen was used as protective atmosphere with a flow rate of 100 ml·min^{-1}.

DPTA monitors the real-time pressure and temperature changes during thermal decomposition by the built-in mini-sensors. A typical DPTA device consists of a program control unit, heating and reaction unit, and data acquisition and processing unit. The detailed components are shown in **Fig. 1**. The test tube loaded with *ca.* 1.0 g of sample was evacuated, and heated to a target temperature at 2 K·min^{-1}, then kept isothermally for 48 h, at last cooled to room temperature. The target temperatures range from 333.15 K to 413.15 K with 20 K increments.
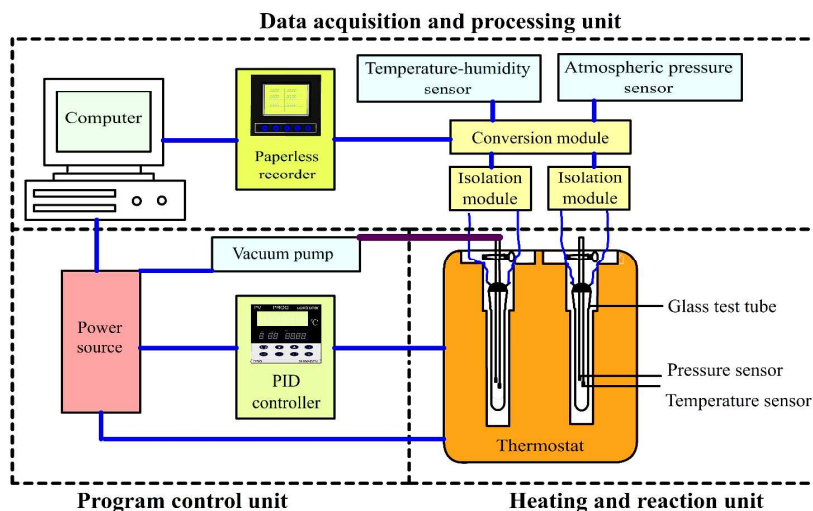

Fig. 1 Schematic diagram of DPTA device

All the tests were carried out at least six times to ensure the accuracy and uncertainty, and the results are the average values of the authentic data.

Results and discussion

Thermal Volatilization

The Antoine equation is an excellent empirical tool for vapor pressure calculation.[35,36]

$$\lg p_{vap} = A - \frac{B}{C+T} \tag{1}$$

where p_{vap} is vapor pressure (Pa), T is absolute temperature (K), A, B, and C are the Antoine constants over a given temperature range and can be referred to literatures.

Assuming that the evaporation/sublimation under isothermal condition is a zero-order process and the free surface area of the sample does not change, the mass loss is caused by evaporation/sublimation and the rate of mass loss is a constant.[31] The sublimation/evaporation parameters can be determined by the rate of mass loss when the sample undergoes a phase transition from solid/liquid to vapor.

The Langmuir equation fits best for determining the vapor pressure from the TG data .[37, 38]

$$\frac{dm}{dt} = p_{vap}\alpha'\sqrt{\frac{M}{2\pi RT}} \tag{2}$$

where dm/dt is volatilization rate *i.e.* mass loss rate (g·s^{-1}), M is molecular mass of vapor (g·mol^{-1}), α' is volatilization

coefficient, and R is the gas constant (8.314 J mol^{-1} K^{-1}).

Rearranging Eq.(2) as follows:

$$p_{vap} = \left(\frac{\sqrt{2\pi R}}{\alpha'} \right) \left(\sqrt{\frac{T}{M}} \frac{dm}{dt} \right) = k_{vap} \cdot v \qquad (3)$$

According to Langmuir, the vaporization coefficient α' is independent of the substance undergoing vaporization, provided the vapor is not associated. The value of α' is stipulated to be equal to 1 in vacuum. Hence, the k_{vap} is also a constant which only depends on the experimental set-up. A plot of p_{vap} (calculated from the Antoine constants) against v (calculated from the TG data) should give a straight line with a slope of k_{vap}. Since the v would be a constant for a given compound, the slope of the p_{vap} vs. v plot would give the value of k_{vap}. Alternatively, if taking the logarithm of Eq.(3), the intercept of the log p_{vap} vs. log v plot would give the value of log k_{vap}. Thus, the vaporization coefficient α' can be determined from the volatilization of one compound which is known to be thermally stable, to follow an ideal behavior for gas–vapor or solid–vapor transitions, and has the known Antoine constants. Benzoic acid has been suggested as a suitable calibration material for this role.[39, 40] Once the k_{vap} value of calibration material is known, the Langmuir equation can be used to determine the vapor pressure of a substance whose Antoine constants have not been characterized.

The TG curves of mass loss vs. time of benzoic acid are shown in **Fig. 2a**, getting the values of dm/dt. The vapor pressures of benzoic acid are calculated based on the Antoine equation (see **Table 2**). The Antoine constants *A, B* and *C* of benzoic acid are referred to the *National Institute of Science and Technology (NIST) Chemistry WebBook* (http://webbook.nist.gov). The Langmuir equation for the evaporation of benzoic acid is determined as shown in **Fig. 3**. The TG curves of TNT, DNAN and DNTF are shown in **Figs. 2b-d**.

(a)   (b)

(c)

(d)
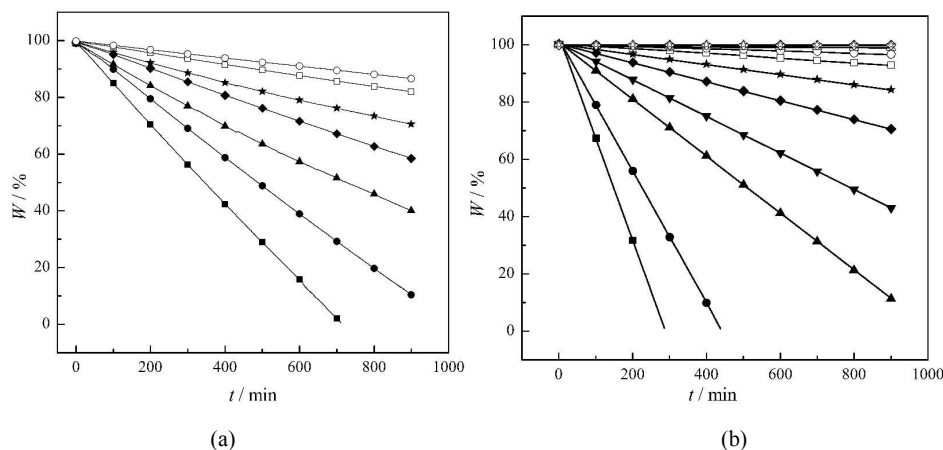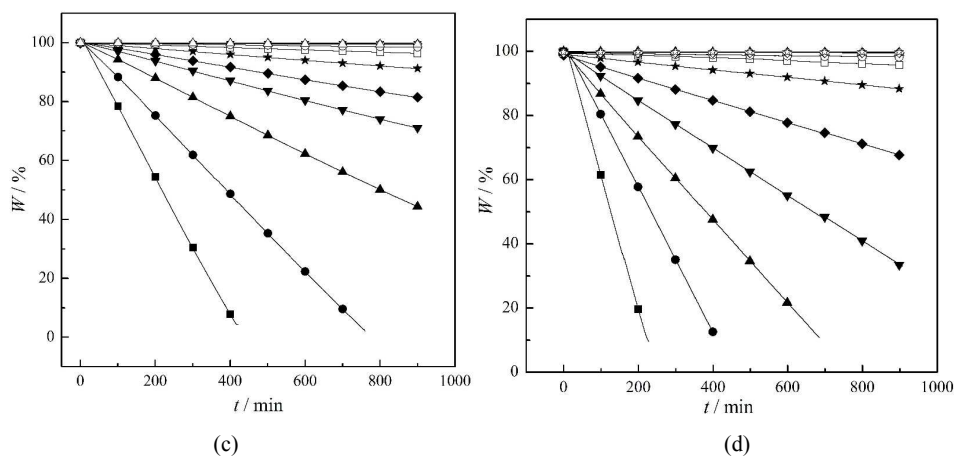
Fig. 2 TG curves of benzoic acid (a) at specified temperatures: ○, T_s=323.15 K; □, T_s =328.15 K; ★, T_s =333.15 K; ◆, T_s =338.15 K; ▲, T_s =343.15 K; ●, T_s =348.15 K; ■, T_s =353.15 K. TG curves of TNT (b), DNAN (c) and DNTF (d) at specified temperatures: □, T_s =323.15 K; □, T_s =333.15 K; □, T_s =343.15 K; ○, T_s =353.15 K; □, T_s =363.15 K; □, T_s =373.15 K; □, T_s =383.15 K; ▼, T_s =393.15 K; ▲, T_s =403.15 K; ●, T_s =413.15 K; ■, T_s =423.15 K.

Table 2 Isothermal TG data of benzoic acid

T_p (K)	n	T (K)	Std. Dev.	dm/dt (μg·min^{-1})	p (Pa)
323.15	54002	332.86	0.0074	1.46	7.08
328.15	54002	337.72	0.0043	1.98	11.29
333.15	54002	341.92	0.0056	3.21	16.71
338.15	54002	346.94	0.0101	4.59	26.36
343.15	54002	351.25	0.0067	6.55	38.60
348.15	54002	356.76	0.0079	9.98	62.00
353.15	42402	360.68	0.0096	13.81	86.10

T_p is programmed temperature, T is actual temperature, n is number of TG data points.

$$p_{vap} = 2.23124\, v - 2.11638$$
$$r = 0.99964$$
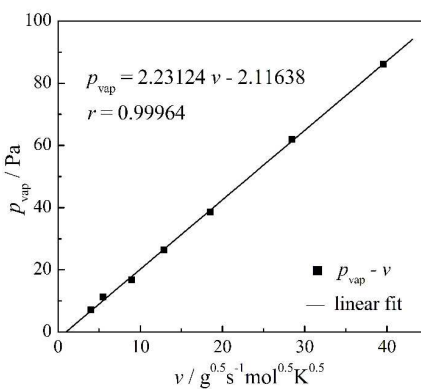
Fig. 3 Langmuir plot for the evaporation of benzoic acid.

The vapor pressures of TNT, DNTF and DNAN at specified temperatures are calculated according to the Langmuir equation (Eq.(3)), and the results are listed in **Table 3**.

The Clausius–Clapeyron equation is used to determine the enthalpies of sublimation and evaporation ($\Delta_{sub}H$ and $\Delta_{vap}H$) in specified temperature ranges. The equation is shown as follows:

$$\lg p_{vap} = Z - \frac{\Delta H}{RT} \qquad (4)$$

where Z is a constant. The value of ΔH is obtained by the slope of the $\lg p$ vs. $1/T$ plot.

According to the Clausius-Clapeyron equation, the enthalpies of sublimation and evaporation ($\Delta_{sub}H$ and $\Delta_{vap}H$) are listed in **Table 3**.

Table 3 Vapor pressures and enthalpies of sublimation and evaporation of TNT, DNAN and DNTF at specified temperatures

Sample	T / K	dm/dt /µg·min^{-1}	p_{vap} / Pa	$\Delta_{sub}H$ / kJ·mol^{-1}	$\Delta_{vap}H$ / kJ·mol^{-1}	r [a]
TNT	324.29	0.007	0.024	144.5	/	-0.9974
	333.38	0.024	0.083			
	342.00	0.076	0.290			
	351.42	0.333	1.469			
	360.46	0.711	3.373	/	89.2	-0.9990
	369.72	1.501	7.649			
	378.87	2.763	14.927			
	388.15	5.302	30.524			
	397.52	8.222	49.386			
	408.30	18.932	123.253			
	417.45	29.233	198.453			
DNAN	324.03	0.006	0.019	124.0	/	-0.9985
	332.83	0.021	0.070			
	342.53	0.069	0.260			
	351.36	0.164	0.677			
	361.08	0.386	1.726			
	370.69	0.940	4.582	/	95.9	-0.9983
	379.87	2.012	10.543			
	388.80	3.131	17.134			
	397.58	6.013	35.035			
	407.74	12.441	77.785			
	416.96	22.633	149.901			
DNTF	324.17	0.004	0.012	133.8	/	-0.9994
	335.00	0.018	0.061			
	342.29	0.049	0.178			
	351.43	0.145	0.591			
	361.47	0.401	1.793			
	370.29	1.122	5.553			
	379.06	3.251	17.856			

388.64	6.870	40.568	/	90.9	-0.9990
398.36	11.933	74.227			
406.77	20.933	137.601			
417.05	38.962	271.941			

[a] r denotes the linear correlation coefficient.

[b] Standard uncertainties u are $u(T) = 0.01$ K, $u(dm/dt) = 0.001$ µg·min^{-1}, and $u(p_{vap}) = 0.005$ Pa.

The increasing sequence of p_{vap} is DNTF < DNAN < TNT below 350 K. Unexpectedly, the p_{vap} of DNTF surpasses that of DNAN at the temperature ranging from 350 K to 380 K, and further surpasses that of TNT with the sequence of DNAN < TNT < DNTF above 380 K. The p_{vap} growth of DNTF is more dramatic than those of the others, which indicates the volatilization of DNTF is most sensitive to heating.

The volatilization process of TNT had been investigated by other methods, and the reported results were listed in **Table 4**.

Table 4 Vapor pressures and enthalpies of sublimation and evaporation of TNT in this work and references

| lg $(p_{vap}$ / Pa)= $A - B$ / $(T$ / K) | | p_{vap} / Pa (298.15 K) | $\Delta_{sub}H$ / kJ·mol^{-1} | Ref. (Author, Year) |
A	B			
16.86	5960	7.33×10^{-4}	114	41 (Edwards, 1950)
13.25	4690		89.8 ($\Delta_{vap}H$)	
17.56	6180	6.56×10^{-4}	118	42 (Pella, 1977)
14.44	5175	1.17×10^{-3}	/	43 (Leggett, 1977)
16.65	5900	7.27×10^{-4}	/	44 (Cundall, 1981)
10.88	4227	5.25×10^{-4}	81	45 (Dobratz, 1985)
5.48	2562	7.50×10^{-4}	113	46 (Dionne, 1986)
20.60	7145	4.17×10^{-4}	137	22 (Oxley, 2005)
		5~15 (373.15 K)		
13.05	4723	1.71×10^{-4}	91	47 (Oxley, 2009)
		14.32 (373.15 K)		
/	/	9.27×10^{-4} [a]	/	15 (Ewing, 2013)
25.81	**9009**	**1.89×10^{-4}**	**144.5**	**This work**
13.46	**4656**	**9.59 (373.15 K)**	**89.2 ($\Delta_{vap}H$)**	

[a] The author calculated the average of six reliable data to get the "best available" value.

The vapor pressures of TNT are determined to 1.89×10^{-4} Pa at 278.15 K and 9.59 Pa at 373.15 K in this work. This result shows good agreement with the reported results within a confidence interval. The $\Delta_{vap}H$ is close to the result from Ref. 41 while the $\Delta_{sub}H$ slightly deviates with one another. Nevertheless, the $\Delta_{sub}H$ is credible in view of the diversity of measuring methods because its relative error to the value of Ref. 22 is less than 10 %.[48]

Thermal Decomposition Behavior

DPTA measured the changes of the apparent evolved gas pressure with time. The interference of the vapor pressure determined by TG was deducted from the apparent evolved gas pressure to obtain the net decomposition gas pressure (p).

The time dependences of the net decomposition gas pressures of TNT, DNAN and DNTF at different temperatures are shown in **Fig. 4**.

(a)   (b)

(c)
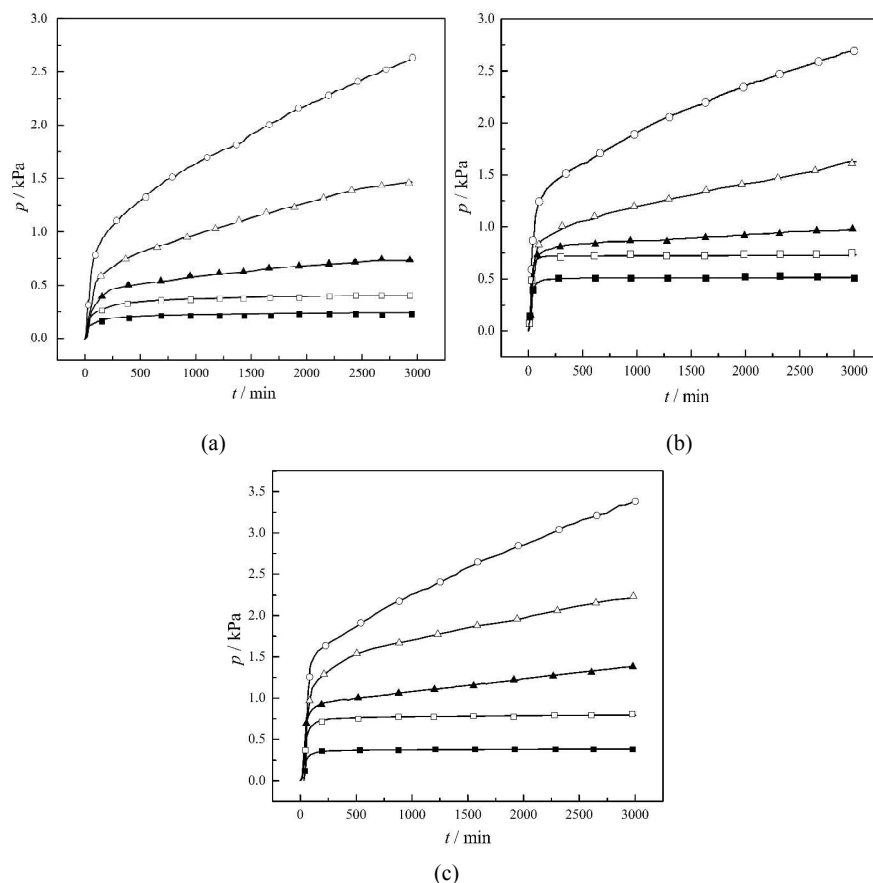
**Fig. 4** Time dependences of decomposition gas pressures of TNT (a), DNAN (b) and DNTF (c) at different temperatures: ■, T=333.15 K; □, T=353.15 K; ▲, T=373.15 K; □, T=393.15 K; ○, T=413.15 K.

The decomposition gas pressures of TNT, DNTF and DNAN all increase significantly with the rise of temperature in the initial non-isothermal stage. The pressures still increase but the growth rate slow gradually in the subsequent isothermal stage. The decomposition undergoes a long-term and smooth process at the last stage. According to the reactions of each sample at different temperatures, the higher temperature leads to the larger amount of decomposition gas. Generally, the decomposition gas volume (V) during isothermal stage is an important criterion of thermal stability for energetic materials.[49, 50] The gas volumes of the LONCs all increase sharply with increasing temperature as shown in **Fig 5**.
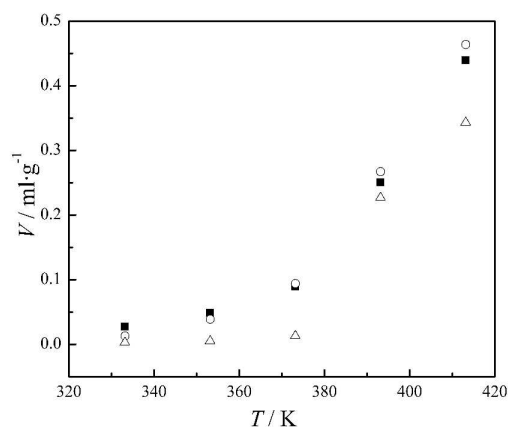
Fig. 5 Decomposition gas volumes of TNT (■), DNAN (□) and DNTF (○) at different temperatures

The less gas volume indicates the better thermal stability. The ascending order of thermal stability conforms to TNT < DNTF < DNAN below 373.15 K but changing to DNTF < TNT < DNAN above 373.15 K. DNAN is the most stable in any case, while DNTF is the most active at high temperature. In summary, TNT, DNTF and DNAN all have excellent thermal stability, because the decomposition gas volumes at 373.15 K are all far less than 2.0 ml·g⁻¹ which is the good stability standard.[51, 52]

Decomposition Kinetics

The non-isothermal kinetic parameters of the LONCs were calculated by means of the universal integral method (UIM) and the differential equation method (DEM).[53]

$$\text{UIM:} \quad \ln\left[\frac{G(\alpha)}{T-T_0}\right] = \ln\frac{A}{\beta} - \frac{E_a}{RT} \quad (5)$$

$$\text{DEM:} \quad \ln\left\{\frac{d\alpha/dT}{f(\alpha)\left[E_a(T-T_0)/(RT^2)+1\right]}\right\} = \ln\frac{A}{\beta} - \frac{E_a}{RT} \quad (6)$$

where $G(\alpha)$ and $f(\alpha)$ are mechanism functions in integral and differential form, respectively, T_0 is initial temperature (K), T is test temperature (K), E_a is apparent activation energy (J·mol⁻¹), A is pre-exponential factor (s⁻¹), β is heating rate (K·min⁻¹), and α is conversion rate of a reaction.

The most probable reaction mechanism (MPRM) was selected from 41 kinds of commonly used mechanisms[53] by the least square method based on the model fitting principle. The corresponding E_a and A were also determined. The results are shown in **Table 5**.

Table 5 Non-isothermal kinetic parameters of TNT, DNAN and DNTF

Sample	UIM				DEM			
	MPRM No. [a]	E_a / kJ·mol⁻¹	lg (A/s^{-1})	r	MPRM No.	E_a / kJ·mol⁻¹	lg (A/s^{-1})	r
TNT	8	105.77	8.73	-0.9972	8	108.76	9.13	-0.9981
DNAN	8	126.50	11.89	-0.9986	8	128.75	12.23	-0.9948

| DNTF | 20 | 99.06 | 8.31 | -0.9934 | 20 | 101.55 | 8.67 | -0.9925 |

[a] For No.8 mechanism, the mechanism functions are $G(\alpha) = [(1+\alpha)^{1/3}-1]^2$ and $f(\alpha) = (3/2)(1+\alpha)^{2/3}[(1+\alpha)^{1/3}-1]^{-1}$. For No.20, $G(\alpha) = [-\ln(1-\alpha)]^4$ and $f(\alpha) = (1/4)(1-\alpha)[-\ln(1-\alpha)]^{-3}$.

[b] Standard uncertainties u are $u(E_a) = 0.01$ kJ·mol^{-1}, and $u(\lg A) = 0.01$ s^{-1}.

The kinetic parameters of each compound calculated by two methods are approximately the same. The MPRMs of TNT and DNAN conform to No.8 mechanism, *i.e.* an Anti-Jander equation described as three-dimensional diffusion. However, the MPRMs of DNTF is No.20 mechanism, *i.e.* an Avrami-Erofeev equation with reaction order $n = 4$ described as random nucleation and subsequent growth. TNT and DNAN have the single benzene ring structure while DNTF has the conjugated furazan and furoxan rings, which could induce the different decomposition mechanisms. The increasing order of E_a is DNTF < TNT < DNAN. E_a represents the energy barrier for the effective collisions among the reactant molecules. The higher value of E_a indicates the higher energy is needed to form the transition state. Therefore, DNAN is much more stable than TNT and DNTF, which coincides with the above result concluded from the decomposition gas volume. The positive correlation between E_a and A is interpreted as the kinetic compensation effect. It suggests that the thermal decompositions of the LONCs are controlled by a common dominant, rate-determining step, resulting in an approximately isokinetic behavior.[54-56] The breakage of C–NO$_2$ could initiate the decomposition of organic nitro compounds in many cases.[57-62]

The isothermal kinetic parameters are calculated using the solid phase reaction kinetic equation.[53]

$$G(\alpha) = k\,t \tag{7}$$

The isothermal MPRM was also selected from 41 mechanisms by the iteration convergence method, and the corresponding reaction rate constants (k) at different temperatures are obtained. The results are listed in **Table 6**.

Table 6 Isothermal kinetic parameters at different temperatures

Sample	T / K [a]	MPRM No. [b]	$10^{-7} \cdot k$ /s^{-1}	r
TNT	333.15	2	2.56	-0.9956
	353.15	2	4.32	-0.9843
	373.15	8	9.54	-0.9798
	393.15	8	17.82	-0.9878
	413.15	8	38.43	-0.9932
DNAN	333.15	9	1.29	-0.9966
	353.15	9	2.88	-0.9749
	373.15	14	6.58	-0.9873
	393.15	14	12.71	-0.9835
	413.15	14	28.40	-0.9984
DNTF	333.15	8	5.88	-0.9679
	353.15	8	9.97	-0.9926
	373.15	25	24.62	-0.9729
	393.15	26	44.20	-0.9873
	413.15	26	65.22	-0.9788

[a] Standard uncertainties u are $u(T) = 0.01$ K, and $u(k) = 0.01 \times 10^{-7}$s^{-1}.

[b] For No.2 mechanism, the mechanism functions are $G(\alpha) = \alpha+(1-\alpha)\ln(1-\alpha)$ and $f(\alpha) = [-\ln(1-\alpha)]^{-1}$. For No.8, $G(\alpha) = [(1+\alpha)^{1/3}-1]^2$ and $f(\alpha) = (3/2)(1+\alpha)^{2/3}[(1+\alpha)^{1/3}-1]^{-1}$. For No.9, $G(\alpha) = [(1-\alpha)^{-1/3}-1]^2$ and $f(\alpha) = (3/2)(1-\alpha)^{4/3}[(1-\alpha)^{-1/3}-1]^{-1}$. For No.14, $G(\alpha) = [-\ln(1-\alpha)]^{-2/3}$ and $f(\alpha) = 3/2(1-\alpha)[-\ln(1-\alpha)]^{-1/3}$. For No.25, $G(\alpha) = \alpha$ and $f(\alpha) = 1$. For No.26, $G(\alpha) =\alpha^{3/2}$ and $f(\alpha) = (2/3)\alpha^{-1/2}$.

The MPRM of each compound vary with temperature. The MPRM of TNT obeys No.2 mechanism *i.e.* a Valensi equation described as two-dimensional diffusion below 373.15 K, then changes to No.8 mechanism above 373.15 K. The MPRM of DNAN changes from No. 9 mechanism to No. 14 mechanism as the temperature increases. That is to say, the MPRM changes from a Zhuralew-Lesokin-Tempelman equantion described as three-dimensional diffusion to an Avrami-Erofeev equation with reaction order $n = 2/3$ described as random nucleation and subsequent growth at the temperature higher than 373.15 K. For DNTF, the MPRM is No. 8 mechanism below 373.15 K, and changes to No.25 mechanism *i.e.* a Mampel powder rule with reaction order $n = 1$ described as one-dimensional phase boundary reaction around 373.15 K. When the temperature exceeds 373.15 K, the MPRM obeys a Mampel power rule with reaction order $n = 3/2$ described as power function. The result indicates the thermal decomposition processes of the LONCs include the complex heterogeneous and multistep reactions.[49, 63-65] The reaction rate constants all rise exponentially as the temperature increases, which indicates that an autocatalytic reaction is involved in the thermal decomposition of LONC.[66-71] The study found that the decomposed products were the porous condensed solids while the reactants are the dispersed particles. It suggests that the LONC melts first and then decomposes as the temperature grows. The surface structure of the condensed matter collapses to form the defects during melting and decomposition.[72, 73] The melted matter obstructs the diffusion of the evolved gases over a brief time. The pores, developing on the reaction interface consequently, potentially become the diffusion channels for the evolved gases and also increase the surface area.[74] The change of the reaction interface could excite more active sites,[75] and accelerate the heat and mass transfer of the reactants and products.[76-79] Therefore, the decomposition of the reactants and the diffusion of the evolved gases are promoted rapidly, and the reaction activity and kinetics are affected. The reaction rate constants arranged from low to high is DNAN < TNT < DNTF, and the growth rate of the reaction rate constant for DNTF is evidently faster than those for the others, as shown in **Fig. 6**.
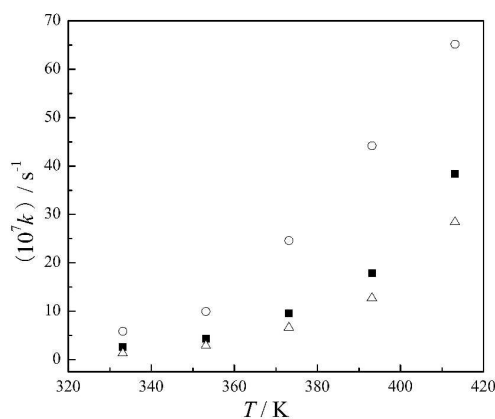

Fig. 6 Reaction rate constants of TNT (■), DNAN (△) and DNTF (○) at different temperatures

This result indicates that the thermal decomposition activity of DNTF is the most sensitive to temperature, which is identical to the volatilization activity. It implies that the activities of volatilization and decomposition are affected by the same factor that is probably the molecular movement rate and collision efficiency. The volatility, thermal stability and kinetic parameters has something to do with the number of the nitro group/nitrogen atom of the LONC molecules, because they conform to the same ascending order of DNAN < TNT < DNTF under specified conditions. Researches show that the nitro compound of the high nitrogen content has the high energy and reaction activity.[80, 81] Therefore, the LONC containing more nitro groups / nitrogen atoms has higher activities of thermal volatilization and thermal decomposition.

Conclusions

The vapor pressures and volatilization enthalpies of three LONCs, TNT, DNAN and DNTF, were determined by TG, and the thermal decomposition behaviors were measured by DPTA. The net gas pressure from thermal decomposition was obtained by quantitatively deducting the vapor pressure from the apparent evolved gas pressure. The thermal decomposition and kinetics prove that DNAN is the most stable, although all LONCs studied showed good thermal stability. . DNTF has the highest reaction activity and most sensitive to heating under specified conditions. The reaction rate constants of the LONC increase with the rise of temperature, which suggests that the thermal decomposition included an autocatalytic reaction and underwent a complex heterogeneous reaction process. The melting and decomposition of the LONC lead to the surface changes which could increase the reaction activity and consequently affect the reaction kinetics and thermal stability. The volatility, thermal stability and kinetic parameters all conform to an identical ascending order under specified conditions that is DNAN < TNT < DNTF. It suggests that the reaction activity of the LONC has a positive correlation with the number of the nitro group/nitrogen atom. Therefore, DNTF has the higher activity and is more sensitive to heating.

Notes and references

* Corresponding author: Tonglai Zhang; e-mail: ztlbit@bit.edu.cn; Tel. & Fax: +8610-68911202; postal address: State Key Laboratory of Explosion Science and Technology, School of Mechatronical Engineering, Beijing Institute of Technology, No. 5, Zhongguancun South Street, Haidian District, Beijing, P. R. China, 100081.

1. V. M. Boddu, K. Abburi, A. J. Fredricksen, S. W. Maloney and R. Damavarapu, *Environ. Technol.*, 2009, **30**, 173-181.

2. V. M. Boddu, K. Abburi, S. W. Maloney and R. Damavarapu, *J. Chem. Eng. Data*, 2008, **53**, 1120-1125.

3. V. P. Sinditskii, V. Y. Egorshev, M. V. Berezin, G. F. Rudakov, A. V. Ladonin and D. V. Katorov, *Propellants, Explos., Pyrotech.*, 2008, **33**, 381-389.

4. A. Provatas and P. J. Davies, *Characterisation of 2,4-dinitroanisole: an ingredient for use in low sensitivity melt cast*

formulations, Weapons Systems Division Defence Science and Technology Organisation, Australia, 2006.

5.   H. X. Hu, Z. Z. Zhang, F. Q. Zhao, C. Xiao, Q. H. Wang and B. H. Yuan, *Acta Armamentarii*, 2004, **25**, 155-158.

6.   V. P. Sinditskii, A. V. Burzhava, A. B. Sheremetev and N. S. Aleksandrova, *Propellants, Explos., Pyrotech.*, 2012, **37**, 575-580.

7.   H.-X. Gao, F.-Q. Zhao, R.-Z. Hu, K.-Z. Xu, H. Zhang, P. Wang, Z.-M. Du, S.-Y. Xu, J.-H. Yi, H.-X. Ma, C.-R. Chang and J.-R. Song, *Chem. J. Chin. Univ.-Chin.*, 2008, **29**, 981-986.

8.   R. Cohen, Y. Zeiri, E. Wurzberg and R. Kosloff, *J. Phys. Chem. A*, 2007, **111**, 11074-11083.

9.   F. Q. Zhao, P. Chen, R. Z. Hu, Y. Luo, Z. Z. Zhang, Y. S. Zhou, X. W. Yang, Y. Gao, S. L. Gao and Q. Z. Shi, *J.Hazard. Mater.*, 2004, **113**, 67-71.

10.   G. Singh, S. P. Felix, D. K. Pandey, J. P. Agrawal and A. K. Sikder, *J. Therm. Anal. Calorim.*, 2005, **79**, 631-635.

11.   J. Andrade, K. Iha, J. A. F. F. Rocco, E. M. Bezerra, M. E. Vazquez Suarez-Iha and G. F. M. Pinheiro, *Quimica Nova*, 2007, **30**, 952-956.

12.   R. K. Tohiani, H. Toghiani, S. W. Maloney and V. M. Boddu, *Fluid Phase Equilib.*, 2008, **264**, 86-92.

13.   J. W. Grate, R. G. Ewing and D. A. Atkinson, *Trac-Trends Anal. Chem.*, 2012, **41**, 1-14.

14.   H. Ostmark, S. Wallin and H. G. Ang, *Propellants, Explos., Pyrotech.*, 2012, **37**, 12-23.

15.   R. G. Ewing, M. J. Waltman, D. A. Atkinson, J. W. Grate and P. J. Hotchkiss, *Trac-Trends Anal. Chem.*, 2013, **42**, 35-48.

16.   M. R. Jerome and D. Charles, *J. Chem. Eng. Data*, 1969, **14**, 120-124.

17.   C. G. Dekruif, T. Kuipers, J. C. Vanmiltenburg, R. C. F. Schaake and G. Stevens, *J. Chem. Thermodyn.*, 1981, **13**, 1081-1086.

18.   P. L. Damour, A. Freedman and J. Wormhoudt, *Propellants, Explos., Pyrotech.*, 2010, **35**, 514-520.

19.   J. L. Goldfarb and E. M. Suuberg, *J. Chem. Thermodyn.*, 2010, **42**, 781-786.

20.   L. Santos, L. Lima, C. Lima, F. D. Magalhaes, M. C. Torres, B. Schroder and M. da Silva, *J. Chem. Thermodyn.*, 2011, **43**, 834-843.

21.   O. V. Surov, M. I. Voronova, N. Z. Mamardashvili and A. G. Zakharov, *Tetrahedron Lett.*, 2011, **52**, 705-707.

22.   J. C. Oxley, J. L. Smith, K. Shinde and J. Moran, *Propellants, Explos., Pyrotech.*, 2005, **30**, 127-130.

23.   D. Lipkind, Y. Kapustin, P. Umnahanant and J. S. Chickos, *Thermochim. Acta*, 2007, **456**, 94-101.

24.   J. S. Chickos, *J. Chem. Eng. Data*, 2010, **55**, 1558-1563.

25.   A. Boller and H. G. Wiedemann, *J. Therm. Anal. Calorim.*, 1998, **53**, 431-439.

26.   A. B. Butrow and R. J. Seyler, *Thermochim. Acta*, 2003, **402**, 145-152.

27.   F. D. Pope, H.-J. Tong, B. J. Dennis-Smither, P. T. Griffiths, S. L. Clegg, J. P. Reid and R. A. Cox, *J. Phys. Chem. A*, 2010, **114**, 10156-10165.

28.   K. Salo, A. M. Jonsson, P. U. Andersson and M. Hallquist, *J. Phys. Chem. A*, 2010, **114**, 4586-4594.

29.   K. Chatterjee, A. Hazra, D. Dollimore and K. S. Alexander, *Eur. J. Pharm. Biopharm.*, 2002, **54**, 171-180.

30.   J. Oxley, J. L. Smith, J. Brady and S. Naik, *Propellants, Explos., Pyrotech.*, 2010, **35**, 278-283.

31.   D. M. Price, *Thermochim. Acta*, 2001, **367**, 253-262.

32.   M. Suceska, S. M. Musanic and I. F. Houra, *Thermochim. Acta*, 2010, **510**, 9-16.

33.   R. Liu, Z. Zhou, Y. Yin, L. Yang and T. Zhang, *Thermochim. Acta*, 2012, **537**, 13-19.

34.   R. Liu, T. Zhang, L. Yang, Z. Zhou and X. Hu, *Cent. Eur. J. Chem.*, 2013, **11**, 774-781.

35.   V. Majer, V. Svoboda and J. Pick, *Heats of Vaporization of Fluids.*, Elsevier, Amsterdam, 1989.

36.   K. Chatterjee, D. Dollimore and K. Alexander, *Int. J. Pharm.*, 2001, **213**, 31-44.

37.   K. Chatterjee, D. Dollimore and K. S. Alexander, *Thermochim. Acta*, 2002, **392**, 107-117.

38.   L. Shen and K. S. Alexander, *Thermochim. Acta*, 1999, **340-341**, 271-278.

39.   S. F. Wright, D. Dollimore, J. G. Dunn and K. Alexander, *Thermochim. Acta*, 2004, **421**, 25-30.

40.   S. F. Wright, P. Phang, D. Dollimore and K. S. Alexander, *Thermochim. Acta*, 2002, **392**, 251-257.

41.   G. Edwards, *Trans. Faraday Soc.*, 1950, **46**, 423.

42.   P. A. Pella, *J. Chem. Thermodyn.*, 1977, **9**, 301.

43.   D. C. Leggett, *J. Chromatogr.*, 1977, **133**, 83.

44.   R. B. Cundall, *J. Chem. Soc.-Faraday Trans. I*, 1981, **77**, 711-712.

45.   B.M.Dobratz and P.L.Crawford, *Explosives Handbook: Principals of Chemical Explosives & Explosive Simulants*, Lawrence

Livermore National Laboratory (LLNL), 1985.

46.   B. C. Dionne, D. P. Roundbehler, E. K. Achter, J. R. Hobbs and D. H. Fine, *J. Energ. Mater.*, 1986, **4**, 447.

47.   J. C. Oxley, J. L. Smith, W. Luo and J. Brady, *Propellants, Explos., Pyrotech.*, 2009, **34**, 539-543.

48.   F. B. Arontini and V. Cozzani, *Thermochim. Acta*, 2007, **460**, 15-21.

49.   M. Chovancova and S. Zeman, *Thermochim. Acta*, 2007, **460**, 67-76.

50.   J. Selesovsky and M. Krupka, 7th International Fall Seminar on Propellants, Explosives and Pyrotechnics, Xi an, China 2007.

51.   GJB 772A-97. Method 501.2: *Vacuum stability test - Method of pressure transducer*, Commission of science technology and industry for national defense: Beijing, 1997, pp 156-158.

52.   GJB 5891.12 - 2006. Test method of loading material for initiating explosive device - Part 12: *Vacuum stability test - Method of pressure transducer,* Commission of science technology and industry for national defense: Beijing, 2006, pp 67-70.,

53.   R. Z. Hu, S. L. Gao, F. Q. Zhao, Q. Z. Shi, T. L. Zhang and J. J. Zhang, Science Press, Beijing, 2008.

54.   P. J. Barrie, *Phys. Chem. Chem. Phys.*, 2012, **14**, 318-326.

55.   P. J. Barrie, *Phys. Chem. Chem. Phys.*, 2012, **14**, 327-336.

56.   J. G. R. Poco, H. Furlan and R. Giudici, *J. Phys. Chem. B*, 2002, **106**, 4873-4877.

57.   Y. Wang, W.-J. Shi, F.-D. Ren, D.-L. Cao and F. Chen, *J. Theor. Comp. Chem.*, 2013, **12**.

58.   Q.-g. Wei, W.-j. Shi, F.-d. Ren, Y. Wang and J. Ren, *J. Mol. Model.*, 2013, **19**, 453-463.

59.   V. L. Korolev, T. S. Pivina, A. A. Porollo, T. V. Petukhova, A. B. Sheremetev and V. P. Ivshin, *Russ. Chem. Rev.*, 2009, **78**, 945-969.

60.   B. Tan, X. Long, R. Peng, H. Li, B. Jin, S. Chu and H. Dong, *J.Hazard. Mater.*, 2010, **183**, 908-912.

61.   X.-F. Chen, J.-F. Liu, Z.-H. Meng and K.-L. Han, *Theor. Chem. Acc.*, 2010, **127**, 327-344.

62.   Q. Wang, J. Wang and M. D. Larranaga, *J. Therm. Anal. Calorim.*, 2013, **111**, 1033-1037.

63.   A. Khawam and D. R. Flanagan, *Thermochim. Acta*, 2005, **429**, 93-102.

64.   S. Vyazovkin, A. K. Burnham, J. M. Criado, L. A. Perez-Maqueda, C. Popescu and N. Sbirrazzuoli, *Thermochim. Acta*, 2011, **520**, 1-19.

65.   C. Danvirutai, P. Noisong and T. Srithanrattana, *J. Therm. Anal. Calorim.*, 2012, **110**, 249-256.

66.   R. G. Sharpe and M. Bowker, *J. Phys.: Condens. Matter*, 1995, **7**, 6379-6392.

67.   Q. L. Yan, S. Zeman, T. L. Zhang and A. Elbeih, *Thermochim. Acta,* 2013, **574**, 10-18.

68.   R. S. Burkina and A. G. Knyazeva, *Comb. Explos. Shock Waves*, 1991, **27**, 143-148.

69.   J. J. Batten, *Int. J. Chem. Kinet.*, 1985, **17**, 1085-1090.

70.   G. T. Long, B. A. Brems and C. A. Wight, *J. Phys. Chem. B*, 2002, **106**, 4022-4026.

71.   R. Behrens, *J. Phys. Chem.*, 1990, **94**, 6706-6718.

72.   N. Koga, Y. Suzuki and T. Tatsuoka, *J. Phys. Chem. B*, 2012, **116**, 14477-14486.

73.   H. Tanaka, N. Koga and A. K. Galwey, *J. Chem. Edu.*, 1995, **72**, 251-256.

74.   T. Wada and N. Koga, *J. Phys. Chem. A*, 2013, **117**, 1880-1889.

75.   N. Koga and H. Tanaka, *J. Phys. Chem.*, 1994, **98**, 10521-10528.

76.   A. S. Rozenberg and E. I. Aleksandrova, *Rus. Chem. Bull.*, 1996, **45**, 64-68.

77.   P. J. Skrdla, *J. Phys. Chem. A*, 2006, **110**, 11494-11500.

78.   P. J. Skrdla and R. T. Robertson, *J. Phys. Chem. B*, 2005, **109**, 10611-10619.

79.   V. I. Levitas, B. F. Henson, L. B. Smilowitz, D. K. Zerkle and B. W. Asay, *J. Appl. Phys.*, 2007, **102**.

80.   T. M. Klaptke, ed. T. M. Klapotke, 2007, vol. 125, pp. 85-121.

81.   D. M. Badgujar, M. B. Talawar, S. N. Asthana and P. P. Mahulikar, *J. Hazard. Mater.*, 2008, **151**, 289-305.